Broadband Achromatic Metalenses in the Visible

Wei Ting Chen[1], **Alexander Y. Zhu**[1], **Vyshakh Sanjeev**[1,2],
Mohammadreza Khorasaninejad[1], **Zhujun Shi**[3], **Eric Lee**[1,2] **and Federico Capasso**[1]

[1]Harvard John A. Paulson School of Engineering and Applied Sciences, Harvard University, Cambridge, Massachusetts 02138, USA
[2]University of Waterloo, Waterloo, ON N2L 3G1, Canada
[3]Department of Physics, Harvard University, Cambridge, Massachusetts 02138, USA

Author e-mail addresses: weitingchen@seas.harvard.edu

Metalenses are planar lenses comprised of sub-wavelength spaced nanostructures that have been demonstrated with many promising applications. However, the control of their dispersion over a large bandwidth has been a challenge. Here, we show that it is possible to realize metalenses with tailored dispersion, including achromatic metalenses over almost the entire visible bandwidth from λ = 470 to 670 nm. This is made possible by simultaneously controlling the phase, group delay and group delay dispersion of an wavefront.

To realize achromatic focusing, we need to impart a target frequency-dependent phase profile: $\varphi(r,\omega) = -\frac{\omega}{c}(\sqrt{r^2+F^2}-F)$, where ω, c, r and F are angular frequency, light speed, lens coordinate and focal length, respectively. This implies that, for a given frequency ω_d, a nanopillar at r needs to be designed to simultaneously satisfy phase delay $\varphi(r,\omega_d)$, group delay $\left.\frac{\partial\varphi}{\partial\omega}\right|_{\omega=\omega_d}$ and group delay dispersion $\left.\frac{\partial^2\varphi}{\partial\omega^2}\right|_{\omega=\omega_d}$. The physical meaning of these terms is schematically shown in Fig. 1(a). Assuming we have an incident wavefront consisting of pulses in the time domain, each pulse, when it passes through different nanopillars (depicted in purple rectangles), experiences different phase delays resulting in a spherical wavefront (yellow line). The pulses also experience various group delays and group delay dispersions such that they reach the focus at the same time and with the same pulse shape. The net effect is to minimize time spread such that all frequency components in the pulse constructively interfere. The smaller the time spread, the larger the bandwidth achievable; an analogue to Heisenberg's uncertainty principle $\Delta E \Delta t \sim \hbar$.

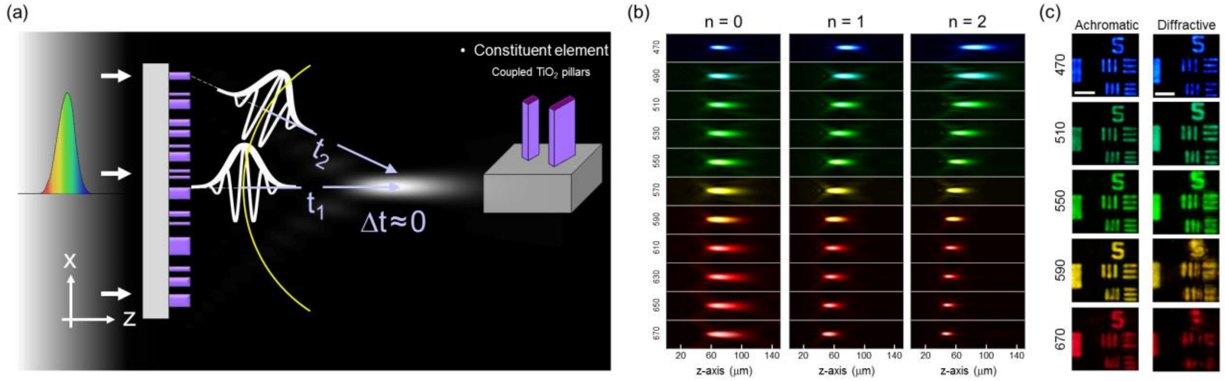

Fig. 1. Dispersion engineering of metalenses. (a) Schematic of an achromatic metalens. The metalens is designed to provide spatially dependent group delays and group delay dispersions such that outgoing wavepackets from different locations are identical and arrive simultaneously at the focus. (b) Measured intensity distributions in linear scale (shown in false colors corresponding to their respective wavelengths) in the x–z plane. The wavelengths of incidence are labeled on the left. These metalenses have a numerical aperture of 0.2 at λ = 530 nm, and a diameter of 25 μm. (c) Images of 1951 United States Air Force resolution target formed by the achromatic (first column) and diffractive (second column) metalenses. Scale bar: 100 μm. The numerical aperture and diameter are 0.02 and 220 μm, respectively.

We placed two TiO_2 nanopillars of different dimensions in close proximity to tune group delay and group delay dispersion through their coupling (inset of Fig. 1(a)). This provides metalenses with tailored focal length shift followed by $F(\omega) = k\omega^n$, where k and n are constants. In Fig. 1(b), we show measured point spread functions of an achromatic metalens (n = 0) and a chromatic metalens (n = 1) whose focal length shift is similar to conventional diffractive lenses. We can further increase the chromatic focal length shift, as seen for the case of n = 2. We also demonstrate an achromatic metalens retaining achromatic imaging from 470 nm to 670 nm compared with its diffractive counterpart (Fig. 1(c)). Additionally, in this talk, I will introduce applications of such dispersion-engineered metalenses. These achromatic and dispersion-tailored metalenses can find numerous applications across industry and scientific research, such as in lithography, microscopy, endoscopy and virtual and augmented reality.